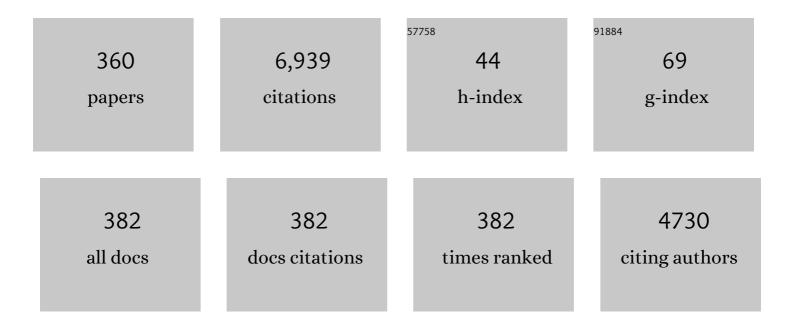
Michael C Kolios

List of Publications by Year in descending order

Source: https://exaly.com/author-pdf/7178709/publications.pdf Version: 2024-02-01



#	Article	IF	CITATIONS
1	A theoretical comparison of energy sources - microwave, ultrasound and laser - for interstitial thermal therapy. Physics in Medicine and Biology, 1998, 43, 3535-3547.	3.0	244
2	Ultrasound imaging of apoptosis: high-resolution non-invasive monitoring of programmed cell death in vitro, in situ and in vivo. British Journal of Cancer, 1999, 81, 520-527.	6.4	194
3	Ultrasonic spectral parameter characterization of apoptosis. Ultrasound in Medicine and Biology, 2002, 28, 589-597.	1.5	177
4	Influence of transition rates and scan rate on kinetic simulations of differential scanning calorimetry profiles of reversible and irreversible protein denaturation. Biochemistry, 1992, 31, 12706-12712.	2.5	168
5	Ultrasound Imaging of Apoptosis in Tumor Response: Novel Preclinical Monitoring of Photodynamic Therapy Effects. Cancer Research, 2008, 68, 8590-8596.	0.9	130
6	Single Cell Photoacoustic Microscopy: A Review. IEEE Journal of Selected Topics in Quantum Electronics, 2016, 22, 137-151.	2.9	126
7	Large blood vessel cooling in heated tissues: a numerical study. Physics in Medicine and Biology, 1995, 40, 477-494.	3.0	125
8	Vaporization of perfluorocarbon droplets using optical irradiation. Biomedical Optics Express, 2011, 2, 1432.	2.9	123
9	Probing Red Blood Cell Morphology Using High-Frequency Photoacoustics. Biophysical Journal, 2013, 105, 59-67.	0.5	118
10	High frequency label-free photoacoustic microscopy of single cells. Photoacoustics, 2013, 1, 49-53.	7.8	116
11	Ultrasonic biomicroscopy of viable, dead and apoptotic cells. Ultrasound in Medicine and Biology, 1997, 23, 961-965.	1.5	114
12	Quantitative Ultrasound Evaluation of Tumor Cell Death Response in Locally Advanced Breast Cancer Patients Receiving Chemotherapy. Clinical Cancer Research, 2013, 19, 2163-2174.	7.0	108
13	Monitoring structural changes in cells with high-frequency ultrasound signal statistics. Ultrasound in Medicine and Biology, 2005, 31, 1041-1049.	1.5	104
14	Ultrasonic Characterization of Whole Cells and Isolated Nuclei. Ultrasound in Medicine and Biology, 2007, 33, 389-401.	1.5	102
15	High-frequency ultrasound scattering from microspheres and single cells. Journal of the Acoustical Society of America, 2005, 117, 934-943.	1.1	96
16	Quantitative Ultrasound Characterization of Responses to Radiotherapy in Cancer Mouse Models. Clinical Cancer Research, 2009, 15, 2067-2075.	7.0	95
17	Blood flow cooling and ultrasonic lesion formation. Medical Physics, 1996, 23, 1287-1298.	3.0	86
18	Contrast enhanced ultrasound imaging by nature-inspired ultrastable echogenic nanobubbles. Nanoscale, 2019, 11, 15647-15658.	5.6	86

#	Article	IF	CITATIONS
19	A simulation study on photoacoustic signals from red blood cells. Journal of the Acoustical Society of America, 2011, 129, 2935-2943.	1.1	80
20	Feasibility of optical coherence elastography measurements of shear wave propagation in homogeneous tissue equivalent phantoms. Biomedical Optics Express, 2012, 3, 972.	2.9	77
21	Quantitative Ultrasound Characterization of Cancer Radiotherapy Effects In Vitro. International Journal of Radiation Oncology Biology Physics, 2008, 72, 1236-1243.	0.8	75
22	Changes in dielectric properties at 460 kHz of kidney and fat during heating: importance for radio-frequency thermal therapy. Physics in Medicine and Biology, 2003, 48, 2509-2525.	3.0	74
23	Quantitative measurements of apoptotic cell properties using acoustic microscopy. IEEE Transactions on Ultrasonics, Ferroelectrics, and Frequency Control, 2010, 57, 2293-2304.	3.0	73
24	Synthesis of Stable Multifunctional Perfluorocarbon Nanoemulsions for Cancer Therapy and Imaging. Langmuir, 2016, 32, 10870-10880.	3.5	73
25	Comparison of thermal damage calculated using magnetic resonance thermometry, with magnetic resonance imaging post-treatment and histology, after interstitial microwave thermal therapy of rabbit brain. Physics in Medicine and Biology, 2000, 45, 3563-3576.	3.0	72
26	High resolution ultrasound and photoacoustic imaging of single cells. Photoacoustics, 2016, 4, 36-42.	7.8	72
27	Photoacoustic ultrasound spectroscopy for assessing red blood cell aggregation and oxygenation. Journal of Biomedical Optics, 2012, 17, 125006.	2.6	68
28	The effects of dynamic optical properties during interstitial laser photocoagulation. Physics in Medicine and Biology, 2000, 45, 1335-1357.	3.0	67
29	A model based upon pseudo regular spacing of cells combined with the randomisation of the nuclei can explain the significant changes in high-frequency ultrasound signals during apoptosis. Ultrasound in Medicine and Biology, 2002, 28, 217-226.	1.5	63
30	Sink or float? Characterization of shell-stabilized bulk nanobubbles using a resonant mass measurement technique. Nanoscale, 2019, 11, 851-855.	5.6	62
31	PMMA-Fe ₃ O ₄ for internal mechanical support and magnetic thermal ablation of bone tumors. Theranostics, 2019, 9, 4192-4207.	10.0	62
32	Magnetic resonance imaging of temperature changes during interstitial microwave heating: A phantom study. Medical Physics, 1997, 24, 269-277.	3.0	61
33	Experimental evaluation of two simple thermal models using transient temperature analysis. Physics in Medicine and Biology, 1998, 43, 3325-3340.	3.0	60
34	Conventional Frequency Ultrasonic Biomarkers of Cancer Treatment Response In Vivo. Translational Oncology, 2013, 6, 234-IN2.	3.7	59
35	Laserâ€Activatible PLGA Microparticles for Imageâ€Guided Cancer Therapy In Vivo. Advanced Functional Materials, 2014, 24, 7674-7680.	14.9	59
36	Low-frequency quantitative ultrasound imaging of cell death <i>in vivo</i> . Medical Physics, 2013, 40, 082901.	3.0	57

#	Article	IF	CITATIONS
37	Objective assessment of stored blood quality by deep learning. Proceedings of the National Academy of Sciences of the United States of America, 2020, 117, 21381-21390.	7.1	57
38	Hybrid Quantum Dotâ~'Fatty Ester Stealth Nanoparticles: Toward Clinically Relevant <i>in Vivo</i> Optical Imaging of Deep Tissue. ACS Nano, 2011, 5, 1958-1966.	14.6	56
39	Influence of the pressure-dependent resonance frequency on the bifurcation structure and backscattered pressure of ultrasound contrast agents: a numerical investigation. Nonlinear Dynamics, 2015, 80, 889-904.	5.2	55
40	Early prediction of therapy responses and outcomes in breast cancer patients using quantitative ultrasound spectral texture. Oncotarget, 2014, 5, 3497-3511.	1.8	55
41	High Frequency Ultrasound Tissue Characterization and Acoustic Microscopy of Intracellular Changes. Ultrasound in Medicine and Biology, 2008, 34, 1396-1407.	1.5	50
42	Speckle statistics in OCT images: Monte Carlo simulations and experimental studies. Optics Letters, 2014, 39, 3472.	3.3	50
43	Quantitative ultrasound radiomics in predicting response to neoadjuvant chemotherapy in patients with locally advanced breast cancer: Results from multiâ€institutional study. Cancer Medicine, 2020, 9, 5798-5806.	2.8	50
44	Detecting apoptosis using dynamic light scattering with optical coherence tomography. Journal of Biomedical Optics, 2011, 16, 070505.	2.6	46
45	On the use of photoacoustics to detect red blood cell aggregation. Biomedical Optics Express, 2012, 3, 2326.	2.9	46
46	Imaging innovations for cancer therapy response monitoring. Imaging in Medicine, 2012, 4, 311-327.	0.0	46
47	Bursting microbubbles: How nanobubble contrast agents can enable the future of medical ultrasound molecular imaging and image-guided therapy. Current Opinion in Colloid and Interface Science, 2021, 54, 101463.	7.4	45
48	Photoacoustic signal characterization of cancer treatment response: Correlation with changes in tumor oxygenation. Photoacoustics, 2017, 5, 25-35.	7.8	44
49	Chemotherapy-Response Monitoring of Breast Cancer Patients Using Quantitative Ultrasound-Based Intra-Tumour Heterogeneities. Scientific Reports, 2017, 7, 10352.	3.3	44
50	Toward Precisely Controllable Acoustic Response of Shell-Stabilized Nanobubbles: High Yield and Narrow Dispersity. ACS Nano, 2021, 15, 4901-4915.	14.6	43
51	Nonlinear dynamics of acoustic bubbles excited by their pressure-dependent subharmonic resonance frequency: influence of the pressure amplitude, frequency, encapsulation and multiple bubble interactions on oversaturation and enhancement of the subharmonic signal. Nonlinear Dynamics, 2021, 103, 429-466.	5.2	42
52	Classification of the nonlinear dynamics and bifurcation structure of ultrasound contrast agents excited at higher multiples of their resonance frequency. Physics Letters, Section A: General, Atomic and Solid State Physics, 2012, 376, 2222-2229.	2.1	41
53	A magnetic droplet vaporization approach using perfluorohexane-encapsulated magnetic mesoporous particles for ultrasound imaging and tumor ablation. Biomaterials, 2017, 134, 43-50.	11.4	41
54	Quantitative ultrasound radiomics for therapy response monitoring in patients with locally advanced breast cancer: Multi-institutional study results. PLoS ONE, 2020, 15, e0236182.	2.5	41

#	Article	IF	CITATIONS
55	Acoustic and photoacoustic characterization of micron-sized perfluorocarbon emulsions. Journal of Biomedical Optics, 2012, 17, 0960161.	2.6	40
56	Delay-encoded transmission and image reconstruction method in synthetic transmit aperture imaging. IEEE Transactions on Ultrasonics, Ferroelectrics, and Frequency Control, 2015, 62, 1745-1756.	3.0	40
57	Collective nonlinear behavior of interacting polydisperse microbubble clusters. Ultrasonics Sonochemistry, 2019, 58, 104708.	8.2	40
58	Ultrasound detection of cell death. Imaging in Medicine, 2010, 2, 17-28.	0.0	37
59	Effects of cell spatial organization and size distribution on ultrasound backscattering. IEEE Transactions on Ultrasonics, Ferroelectrics, and Frequency Control, 2011, 58, 2118-2131.	3.0	37
60	Modeling photoacoustic spectral features of micron-sized particles. Physics in Medicine and Biology, 2014, 59, 5795-5810.	3.0	37
61	High-frequency ultrasound for monitoring changes in liver tissue during preservation. Physics in Medicine and Biology, 2005, 50, 197-213.	3.0	36
62	An Increase in Cellular Size Variance Contributes to the Increase in Ultrasound Backscatter During Cell Death. Ultrasound in Medicine and Biology, 2010, 36, 1546-1558.	1.5	36
63	Quantitative Ultrasound for the Monitoring of Novel Microbubble and Ultrasound Radiosensitization. Ultrasound in Medicine and Biology, 2012, 38, 1212-1221.	1.5	35
64	Biodegradable polymeric nanoparticles containing gold nanoparticles and Paclitaxel for cancer imaging and drug delivery using photoacoustic methods. Biomedical Optics Express, 2016, 7, 4125.	2.9	33
65	Wide dynamic range detection of bidirectional flow in Doppler optical coherence tomography using a two-dimensional Kasai estimator. Optics Letters, 2007, 32, 253.	3.3	32
66	Study of laser-induced thermoelastic deformation of native and coagulated ex-vivo bovine liver tissues for estimating their optical and thermomechanical properties. Journal of Biomedical Optics, 2010, 15, 065002.	2.6	32
67	Detecting cell death with optical coherence tomography and envelope statistics. Journal of Biomedical Optics, 2011, 16, 026017.	2.6	32
68	An investigation of the flow dependence of temperature gradients near large vessels during steady state and transient tissue heating. Physics in Medicine and Biology, 1999, 44, 1479-1497.	3.0	31
69	A simple method to analyze the super-harmonic and ultra-harmonic behavior of the acoustically excited bubble oscillator. Ultrasonics Sonochemistry, 2019, 54, 99-109.	8.2	31
70	Classification of the major nonlinear regimes of oscillations, oscillation properties, and mechanisms of wave energy dissipation in the nonlinear oscillations of coated and uncoated bubbles. Physics of Fluids, 2021, 33, .	4.0	31
71	Magnetic nanoparticle-promoted droplet vaporization for in vivo stimuli-responsive cancer theranostics. NPG Asia Materials, 2016, 8, e313-e313.	7.9	30
72	Stable microfluidic flow focusing using hydrostatics. Biomicrofluidics, 2017, 11, 034104.	2.4	30

#	Article	IF	CITATIONS
73	Simultaneous acoustic and photoacoustic microfluidic flow cytometry for label-free analysis. Scientific Reports, 2019, 9, 1585.	3.3	30
74	Photoacoustic Imaging of Cancer Treatment Response: Early Detection of Therapeutic Effect from Thermosensitive Liposomes. PLoS ONE, 2016, 11, e0165345.	2.5	30
75	Potential use of ultrasound for the detection of cell changes in cancer treatment. Future Oncology, 2009, 5, 1527-1532.	2.4	29
76	Classification of blood cells and tumor cells using labelâ€free ultrasound and photoacoustics. Cytometry Part A: the Journal of the International Society for Analytical Cytology, 2015, 87, 741-749.	1.5	29
77	Intrinsically absorbing photoacoustic and ultrasound contrast agents for cancer therapy and imaging. Nanotechnology, 2018, 29, 505103.	2.6	29
78	Nonlinear power loss in the oscillations of coated and uncoated bubbles: Role of thermal, radiation and encapsulating shell damping at various excitation pressures. Ultrasonics Sonochemistry, 2020, 66, 105070.	8.2	29
79	Nonlinear dynamics and bifurcation structure of ultrasonically excited lipid coated microbubbles. Ultrasonics Sonochemistry, 2021, 72, 105405.	8.2	28
80	Effects of erythrocyte oxygenation on optoacoustic signals. Journal of Biomedical Optics, 2011, 16, 115003.	2.6	27
81	Theoretical and Experimental Gas Volume Quantification of Micro- and Nanobubble Ultrasound Contrast Agents. Pharmaceutics, 2020, 12, 208.	4.5	27
82	Investigating longitudinal changes in the mechanical properties of MCF-7 cells exposed to paclitaxol using particle tracking microrheology. Physics in Medicine and Biology, 2013, 58, 923-936.	3.0	26
83	Quantification of Ultrasonic Scattering Properties of In Vivo Tumor Cell Death in Mouse Models of Breast Cancer. Translational Oncology, 2015, 8, 463-473.	3.7	26
84	The fluid and elastic nature of nucleated cells: Implications from the cellular backscatter response. Journal of the Acoustical Society of America, 2007, 121, EL16-EL22.	1.1	25
85	The measurement of ultrasound scattering from individual micron-sized objects and its application in single cell scattering. Journal of the Acoustical Society of America, 2010, 128, 894-902.	1.1	25
86	Improving the quality of photoacoustic images using the short-lag spatial coherence imaging technique. Proceedings of SPIE, 2013, , .	0.8	25
87	Optical coherence tomography detection of shear wave propagation in inhomogeneous tissue equivalent phantoms and ex-vivo carotid artery samples. Biomedical Optics Express, 2014, 5, 895.	2.9	25
88	Near-infrared absorbing nanoemulsions as nonlinear ultrasound contrast agents for cancer theranostics. Journal of Molecular Liquids, 2019, 287, 110848.	4.9	25
89	Insights into photoacoustic speckle and applications in tumor characterization. Photoacoustics, 2019, 14, 37-48.	7.8	25
90	Determination of cell nucleus-to-cytoplasmic ratio using imaging flow cytometry and a combined ultrasound and photoacoustic technique: a comparison study. Journal of Biomedical Optics, 2019, 24, 1.	2.6	25

#	Article	IF	CITATIONS
91	Ultrasound Imaging of Apoptosis: Spectroscopic Detection of DNA-Damage Effects at High and Low Frequencies. Methods in Molecular Biology, 2011, 682, 165-187.	0.9	24
92	Photoacoustic imaging of kidney fibrosis for assessing pretransplant organ quality. JCI Insight, 2020, 5, .	5.0	24
93	Monitoring of Cell Death in Epithelial Cells Using High Frequency Ultrasound Spectroscopy. Ultrasound in Medicine and Biology, 2009, 35, 482-493.	1.5	23
94	High-Frequency Acoustic Impedance Imaging of Cancer Cells. Ultrasound in Medicine and Biology, 2015, 41, 2700-2713.	1.5	22
95	Critical corrections to models of nonlinear power dissipation of ultrasonically excited bubbles. Ultrasonics Sonochemistry, 2020, 66, 105089.	8.2	22
96	Optoacoustic characterization of prostate cancer in an <i>in vivo</i> transgenic murine model. Journal of Biomedical Optics, 2014, 19, 056008.	2.6	21
97	An investigation of the use of transmission ultrasound to measure acoustic attenuation changes in thermal therapy. Medical and Biological Engineering and Computing, 2006, 44, 583-591.	2.8	20
98	Photoacoustic detection and optical spectroscopy of high-intensity focused ultrasound-induced thermal lesions in biologic tissue. Medical Physics, 2014, 41, 053502.	3.0	20
99	Properties of cells through life and death – an acoustic microscopy investigation. Cell Cycle, 2015, 14, 2891-2898.	2.6	20
100	Microfluidic Generation of Monodisperse Nanobubbles by Selective Gas Dissolution. Small, 2021, 17, e2100345.	10.0	20
101	Multifunctional nanoparticles as theranostic agents for therapy and imaging of breast cancer. Journal of Photochemistry and Photobiology B: Biology, 2021, 218, 112110.	3.8	20
102	Validity of a theoretical model to examine blood oxygenation dependent optoacoustics. Journal of Biomedical Optics, 2012, 17, 055002.	2.6	19
103	Pickering Bubbles as Dual-Modality Ultrasound and Photoacoustic Contrast Agents. ACS Applied Materials & Interfaces, 2020, 12, 22308-22317.	8.0	19
104	Experimental and numerical evidence of intensified non-linearity at the microscale: The lipid coated acoustic bubble. Physics of Fluids, 2021, 33, .	4.0	19
105	Simultaneous assessment of red blood cell aggregation and oxygen saturation under pulsatile flow using high-frequency photoacoustics. Biomedical Optics Express, 2016, 7, 2769.	2.9	18
106	Simultaneous ultra-high frequency photoacoustic microscopy and photoacoustic radiometry of zebrafish larvae in vivo. Photoacoustics, 2018, 12, 14-21.	7.8	18
107	Photoacoustic F-Mode imaging for scale specific contrast in biological systems. Communications Physics, 2019, 2, .	5.3	18
108	Sizing biological cells using a microfluidic acoustic flow cytometer. Scientific Reports, 2019, 9, 4775.	3.3	18

#	Article	IF	CITATIONS
109	Biomedical nanobubbles and opportunities for microfluidics. RSC Advances, 2021, 11, 32750-32774.	3.6	18
110	Comparison of methods for texture analysis of QUS parametric images in the characterization of breast lesions. PLoS ONE, 2020, 15, e0244965.	2.5	18
111	Non-invasive Monitoring of Ultrasound-Stimulated Microbubble Radiation Enhancement Using Photoacoustic Imaging. TCRT Express, 2014, 13, 435-44.	1.5	17
112	Assessment of the Nucleus-to-Cytoplasmic Ratio in MCF-7 Cells Using Ultra-high Frequency Ultrasound and Photoacoustics. International Journal of Thermophysics, 2016, 37, 1.	2.1	17
113	Dosage-controlled intracellular delivery mediated by acoustofluidics for lab on a chip applications. Lab on A Chip, 2021, 21, 1788-1797.	6.0	17
114	A tutorial in photoacoustic microscopy and tomography signal processing methods. Journal of Applied Physics, 2021, 129, .	2.5	17
115	Photoacoustic field calculation for nonspherical axisymmetric fluid particles. Biomedical Physics and Engineering Express, 2017, 3, 015017.	1.2	16
116	Low-power noncontact photoacoustic microscope for bioimaging applications. Journal of Biomedical Optics, 2017, 22, 046001.	2.6	16
117	Labelâ€Free Analysis of Red Blood Cell Storage Lesions Using Imaging Flow Cytometry. Cytometry Part A: the Journal of the International Society for Analytical Cytology, 2019, 95, 976-984.	1.5	16
118	Photoacoustic imaging biomarkers for monitoring biophysical changes during nanobubble-mediated radiation treatment. Photoacoustics, 2020, 20, 100201.	7.8	16
119	Opto-acoustic imaging of relative blood oxygen saturation and total hemoglobin for breast cancer diagnosis. Journal of Biomedical Optics, 2019, 24, 1.	2.6	16
120	Temperature dependence of acoustic harmonics generated by nonlinear ultrasound wave propagation in water at various frequencies. Journal of the Acoustical Society of America, 2016, 139, 2475-2481.	1.1	15
121	Perfluorocarbon bubbles as photoacoustic signal amplifiers for cancer theranostics. Optical Materials Express, 2019, 9, 4532.	3.0	15
122	Sound velocity and attenuation measurements of perfluorocarbon liquids using photoacoustic methods. , 2011, , .		14
123	Temperature dependence of acoustic harmonics generated by nonlinear ultrasound beam propagation in <i>ex vivo</i> tissue and tissue-mimicking phantoms. International Journal of Hyperthermia, 2015, 31, 666-673.	2.5	14
124	Honey, I shrunk the bubbles: microfluidic vacuum shrinkage of lipid-stabilized microbubbles. Soft Matter, 2017, 13, 4011-4016.	2.7	14
125	<i>In vitro</i> photoacoustic spectroscopy of pulsatile blood flow: Probing the interrelationship between red blood cell aggregation and oxygen saturation. Journal of Biophotonics, 2018, 11, e201700300.	2.3	14
126	Ultrasound Imaging of Apoptosis: DNA-Damage Effects Visualized. , 2002, 203, 257-277.		13

#	Article	IF	CITATIONS
127	A study of high frequency ultrasound scattering from non-nucleated biological specimens. Journal of the Acoustical Society of America, 2008, 124, EL278-EL283.	1.1	13
128	Detecting abnormal vasculature from photoacoustic signals using wavelet-packet features. Proceedings of SPIE, 2011, , .	0.8	13
129	Quantitative Ultrasound Spectroscopic Imaging for Characterization of Disease Extent in Prostate Cancer Patients. Translational Oncology, 2015, 8, 25-34.	3.7	13
130	Pseudoinverse Decoding Process in Delay-Encoded Synthetic Transmit Aperture Imaging. IEEE Transactions on Ultrasonics, Ferroelectrics, and Frequency Control, 2016, 63, 1372-1379.	3.0	13
131	On the threshold of 1/2 order subharmonic emissions in the oscillations of ultrasonically excited bubbles. Ultrasonics, 2021, 112, 106363.	3.9	13
132	Dynamic light scattering optical coherence tomography to probe motion of subcellular scatterers. Journal of Biomedical Optics, 2019, 24, 1.	2.6	13
133	High-frequency ultrasound detection of cell death: Spectral differentiation of different forms of cell death in vitro. Oncoscience, 2016, 3, 275-287.	2.2	12
134	Dancing with the Cells: Acoustic Microflows Generated by Oscillating Cells. Small, 2020, 16, 1903788.	10.0	12
135	Use of photoacoustic imaging for monitoring vascular disrupting cancer treatments. Journal of Biophotonics, 2023, 16, e202000209.	2.3	12
136	Laser activatable perfluorocarbon bubbles for imaging and therapy through enhanced absorption from coupled silica coated gold nanoparticles. RSC Advances, 2021, 11, 4906-4920.	3.6	12
137	High frequency optoacoustic microscopy. , 2009, 2009, 5883-6.		11
138	Optoacoustic signal amplitude and frequency spectrum analysis laser heated bovine liver ex vivo. , 2011, , .		11
139	Surface modes and acoustic scattering of microspheres and ultrasound contrast agents. Journal of the Acoustical Society of America, 2012, 132, 1820-1829.	1.1	11
140	Fluence-matching technique using photoacoustic radiofrequency spectra for improving estimates of oxygen saturation. Photoacoustics, 2020, 19, 100182.	7.8	11
141	Measuring the mechanical properties of cells using acoustic microscopy. , 2009, 2009, 6042-5.		10
142	Evaluating the extent of cell death in 3D high frequency ultrasound by registration with	3.0	10
143	Photoacoustic Microscopy and Spectroscopy of Individual Red Blood Cells. , 2010, , .		10
144	Gigahertz optoacoustic imaging for cellular imaging. Proceedings of SPIE, 2010, , .	0.8	10

#	Article	IF	CITATIONS
145	Shrinking microbubbles with microfluidics: mathematical modelling to control microbubble sizes. Soft Matter, 2017, 13, 8796-8806.	2.7	10
146	An artificially engineered "tumor bio-magnet―for collecting blood-circulating nanoparticles and magnetic hyperthermia. Biomaterials Science, 2019, 7, 1815-1824.	5.4	10
147	MRI texture features from tumor core and margin in the prediction of response to neoadjuvant chemotherapy in patients with locally advanced breast cancer. Oncotarget, 2021, 12, 1354-1365.	1.8	10
148	Noninvasive calibrated tissue temperature estimation using backscattered energy of acoustic harmonics. Ultrasonics, 2021, 114, 106406.	3.9	10
149	Expansion-mediated breakup of bubbles and droplets in microfluidics. Physical Review Fluids, 2020, 5, .	2.5	10
150	Optical droplet vaporization (ODV): Photoacoustic characterization of perfluorocarbon droplets. , 2010, , .		9
151	Photoacoustic cardiovascular imaging: a new technique for imaging of atherosclerosis and vulnerable plaque detection. Biomedical Physics and Engineering Express, 2018, 4, 032002.	1.2	9
152	In situ forming implants exposed to ultrasound enhance therapeutic efficacy in subcutaneous murine tumors. Journal of Controlled Release, 2020, 324, 146-155.	9.9	9
153	Anti-HER2 PLGA-PEG polymer nanoparticle containing gold nanorods and paclitaxel for laser-activated breast cancer detection and therapy. Biomedical Optics Express, 2021, 12, 2171.	2.9	9
154	Towards understanding the nature of high frequency backscatter from cells and tissues: an investigation of backscatter power spectra from different concentrations of cells of different sizes. , 0, , .		8
155	Photoacoustic detection of protein coagulation in albumen-based phantoms. Proceedings of SPIE, 2008, , .	0.8	8
156	PLGA/PFC particles loaded with gold nanoparticles as dual contrast agents for photoacoustic and ultrasound imaging. , 2014, , .		8
157	Feasibility of detecting change in backscattered energy of acoustic harmonics in locally heated tissues. International Journal of Hyperthermia, 2019, 36, 963-973.	2.5	8
158	Optical and photoacoustic radiofrequency spectroscopic analysis for detecting red blood cell death. Journal of Biophotonics, 2019, 12, e201800431.	2.3	8
159	The dance of the nanobubbles: detecting acoustic backscatter from sub-micron bubbles using ultra-high frequency acoustic microscopy. Nanoscale, 2020, 12, 21420-21428.	5.6	8
160	<i>A priori</i> prediction of response in multicentre locally advanced breast cancer (LABC) patients using quantitative ultrasound and derivative texture methods. Oncotarget, 2021, 12, 81-94.	1.8	8
161	Radiomics in predicting recurrence for patients with locally advanced breast cancer using quantitative ultrasound. Oncotarget, 2021, 12, 2437-2448.	1.8	8
162	Using high frequency ultrasound envelope statistics to determine scatterer number density in dilute cell solutions. , 0, , .		7

#	Article	IF	CITATIONS
163	Assessment of opto-mechanical behavior of biological samples by interferometry. Proceedings of SPIE, 2009, , .	0.8	7
164	Optical droplet vaporization of micron-sized perfluorocarbon droplets and their photoacoustic detection. , 2011, , .		7
165	Photoacoustic measurements of single red blood cells. , 2012, , .		7
166	Photoacoustic tissue characterization using envelope statistics and ultrasonic spectral parameters. Proceedings of SPIE, 2014, , .	0.8	7
167	Optical coherence tomography spectral analysis for detecting apoptosis <i>in vitro</i> and <i>in vivo</i> . Journal of Biomedical Optics, 2015, 20, 126001.	2.6	7
168	Classification of biological cells using a sound wave based flow cytometer. Proceedings of SPIE, 2016,	0.8	7
169	Triplex micron-resolution acoustic, photoacoustic, and optical transmission microscopy via photoacoustic radiometry. Optics Express, 2018, 26, 22315.	3.4	7
170	Real-Time Control of Nanoparticle-Mediated Thermal Therapy Using Photoacoustic Imaging. IEEE Transactions on Biomedical Engineering, 2021, 68, 2188-2194.	4.2	7
171	A Theoretical Model for RF Ablation of Kidney Tissue and Its Experimental Validation. Lecture Notes in Computer Science, 2010, , 119-129.	1.3	7
172	Photoacoustic simulations of microvascular bleeding: spectral analysis and its application for monitoring vascular-targeted treatments. Journal of Biomedical Optics, 2019, 24, 1.	2.6	7
173	High-frequency ultrasound analysis of post-mitotic arrest cell death. Oncoscience, 2016, 3, 109-121.	2.2	7
174	The role of primary and secondary delays in the effective resonance frequency of acoustically interacting microbubbles. Ultrasonics Sonochemistry, 2022, 86, 106033.	8.2	7
175	<title>Ultrasound backscatter microscopy/spectroscopy and optical coherence (Doppler) tomography for mechanism-specific monitoring of photodynamic therapy in vivo and in vitro</title> . , 2002, , .		6
176	Attenuation mapping for monitoring thermal therapy using ultrasound transmission imaging. , 2004, 2004, 1329-32.		6
177	Visualization of apoptotic cells using scanning acoustic microscopy and high frequency ultrasound. , 2005, , .		6
178	Quantifying the ultrasonic properties of cells during apoptosis using time resolved acoustic microscopy. , 2009, , .		6
179	Optoacoustic detection of thermal lesions. Proceedings of SPIE, 2009, , .	0.8	6
180	Development of a microfluidic device with integrated high frequency ultrasound probe for particle characterization. , 2014, , .		6

#	Article	IF	CITATIONS
181	Nonlinear model of acoustical attenuation and speed of sound in a bubbly medium. , 2015, , .		6
182	Investigation of the nonlinear propagation of ultrasound through a bubbly medium including multiple scattering and bubble-bubble interaction: Theory and experiment. , 2017, , .		6
183	In vivo photoacoustic assessment of the oxygen saturation changes in the human radial artery: a preliminary study associated with age. Journal of Biomedical Optics, 2021, 26, .	2.6	6
184	Probing Different Biological Length Scales Using Photoacoustics: From 1 To 1000 MHz. , 2014, , 1-18.		6
185	Optoacoustic imaging of an animal model of prostate cancer. , 2010, , .		5
186	Ultrasonic characterization of extra-cellular matrix in decellularized murine kidney and liver. , 2015, ,		5
187	Exact solution for a photoacoustic wave from a finite-length cylindrical source. Journal of the Acoustical Society of America, 2015, 137, 1675-1682.	1.1	5
188	Spatial interference encoding patterns based photoacoustic microscopy. Optics Communications, 2017, 401, 23-28.	2.1	5
189	Preliminary photoacoustic imaging of the human radial artery for simultaneous assessment of red blood cell aggregation and oxygen saturation in vivo. , 2017, , .		5
190	Mean Scatterer Spacing Estimation Using Cepstrum-Based Continuous Wavelet Transform. IEEE Transactions on Ultrasonics, Ferroelectrics, and Frequency Control, 2020, 67, 1118-1126.	3.0	5
191	Emerging use of machine learning and advanced technologies to assess red cell quality. Transfusion and Apheresis Science, 2020, 59, 103020.	1.0	5
192	In vivo spectroscopic photoacoustic imaging and laserâ€induced nanoparticle vaporization for antiâ€HER2 breast cancer. Journal of Biophotonics, 2021, 14, e202100099.	2.3	5
193	Experimental design and numerical investigation of a photoacoustic sensor for a low-power, continuous-wave, laser-based frequency-domain photoacoustic microscopy. Journal of Biomedical Optics, 2019, 24, 1.	2.6	5
194	High-Frequency Ultrasound Assessment of Antimicrobial Photodynamic Therapy In Vitro. Journal of Biological Physics, 2007, 33, 61-66.	1.5	4
195	Optical coherence tomography speckle decorrelation for detecting cell death. Proceedings of SPIE, 2011, , .	0.8	4
196	Detection and characterization of higher order nonlinearities in the oscillations of Definity at higher frequencies and very low acoustic pressures. , 2012, , .		4
197	Detection and characterization of red blood cell (RBC) aggregation with photoacoustics. Proceedings of SPIE, 2012, , .	0.8	4
198	The utilization of the bubble pressure dependent harmonic resonance frequency for enhanced heating during high intensity focused ultrasound treatments. AIP Conference Proceedings, 2012, , .	0.4	4

#	Article	IF	CITATIONS
199	Quantitative ultrasound analyses of cell starvation in HT-29 pellets. , 2014, , .		4
200	Mean scatterer spacing estimation from pellets using cepstral analysis: A preliminary study. , 2015, , .		4
201	Monitoring Quantitative Ultrasound Parameter Changes in a Cell Pellet Model of Cell Starvation. Biophysical Journal, 2017, 112, 2634-2640.	0.5	4
202	Ultrasound signal from sub-micron lipid-coated bubbles. , 2017, , .		4
203	Feasibility of photoacoustic imaging for the nonâ€invasive quality management of stored blood bags. Vox Sanguinis, 2019, 114, 701-710.	1.5	4
204	Large-Pitch Synthetic Transmit Aperture Imaging: A Feasibility Study. IEEE Transactions on Ultrasonics, Ferroelectrics, and Frequency Control, 2020, 67, 1317-1331.	3.0	4
205	An image-based flow cytometric approach to the assessment of the nucleus-to-cytoplasm ratio. PLoS ONE, 2021, 16, e0253439.	2.5	4
206	Application of image flow cytometry for the characterization of red blood cell morphology. Proceedings of SPIE, 2017, , .	0.8	4
207	Effect of chromatin structure on quantitative ultrasound parameters. Oncotarget, 2017, 8, 19631-19644.	1.8	4
208	High frequency ultrasound in monitoring liver suitability for transplantation. , 0, , .		3
209	The effect of volume fraction on the backscatter from nucleated cells at high frequencies. , 0, , .		3
210	A comparison of cellular ultrasonic properties during apoptosis and mitosis using acoustic microscopy. , 2010, , .		3
211	Dynamics of laser induced thermoelastic expansion of native and coagulated ex-vivo soft tissue samples and their optical and thermo-mechanical properties. , 2011, , .		3
212	Ultrasound drug targeting to tumors with thermosensitive liposomes. , 2011, , .		3
213	Measuring intracellular motion using dynamic light scattering with optical coherence tomography in a mouse tumor model. Proceedings of SPIE, 2012, , .	0.8	3
214	Photoacoustic spectral characterization of perfluorocarbon droplets. , 2012, , .		3
215	Photoacoustic radio-frequency spectroscopy (PA-RFS): A technique for monitoring absorber size and concentration. , 2013, , .		3
216	Bifurcation structure of the ultrasonically excited microbubbles undergoing buckling and rupture. Proceedings of Meetings on Acoustics, 2013, , .	0.3	3

#	Article	IF	CITATIONS
217	Delay-encoded transmission in synthetic transmit aperture (DE-STA) imaging. , 2014, , .		3
218	Personalization of breast cancer chemotherapy using noninvasive imaging methods to detect tumor cell death responses. Breast Cancer Management, 2014, 3, 31-35.	0.2	3
219	Simulation studies of filtered spatial compounding (FSC) and filtered frequency compounding (FFC) in synthetic transmit aperture (STA) imaging. , 2015, , .		3
220	Differentiation between cellularized and decellularized mouse kidneys using mean scatterer spacing: A preliminary study. , 2016, , .		3
221	Simultaneous photoacoustic and optical attenuation imaging of single cells using photoacoustic microscopy. Proceedings of SPIE, 2016, , .	0.8	3
222	Quantitative photoacoustic assessment of red blood cell aggregation under pulsatile blood flow: experimental and theoretical approaches. Proceedings of SPIE, 2017, , .	0.8	3
223	Opto-Acoustic Image Reconstruction and Motion Tracking Using Convex Optimization. IEEE Transactions on Computational Imaging, 2021, 7, 1161-1175.	4.4	3
224	Probing Different Biological Length Scales Using Photoacoustics: From 1 to 1000 MHz. , 2017, , 303-324.		3
225	Characterization of red blood cell aggregation with photoacoustics: A theoretical and experimental study. , 2011, , .		2
226	Optimization of the shear stress induced by ultrasonically-stimulated oscillating MBs: A theoretical investigation. , 2012, , .		2
227	A photoacoustic technique to measure the properties of single cells. , 2013, , .		2
228	Longitudinal monitoring of oxygen saturation with photoacoustic imaging. , 2014, , .		2
229	Comparison of different image reconstruction algorithms for synthetic transmit aperture imaging using sparse receiving array. , 2014, , .		2
230	Laser-activated PLGA theranostic agents for cancer therapy in vivo. , 2014, , .		2
231	Assessing storage-induced red blood cell lesions using photoacoustic measurements of oxygen saturation and the frequency content of photoacoustic signals. , 2014, , .		2
232	Quantifying temperature changes in tissue-mimicking fluid phantoms using optical coherence tomography and envelope statistics. , 2014, , .		2
233	Probing the in vivo changes in oxygen saturation with photoacoustic imaging as a non-invasive means of assessing treatment progression. Proceedings of SPIE, 2015, , .	0.8	2
234	Evaluation of the morphological parameters of cancer cells using high-frequency ultrasound and photoacoustics. , 2015, , .		2

#	Article	IF	CITATIONS
235	Numerical investigation of plasmonic properties of gold nanoshells. , 2015, , .		2
236	Gold-nanoshells as surface plasmon resonance (SPR). , 2015, , .		2
237	Effect of optical wavelength on photoacoustic investigations of pulsatile blood flow. Proceedings of SPIE, 2016, , .	0.8	2
238	In Vitro Studies of Multifunctional Perfluorocarbon Nanoemulsions for Cancer Therapy and Imaging. Biophysical Journal, 2016, 110, 503a.	0.5	2
239	High frequency ultrasound imaging and simulations of sea urchin oocytes. Journal of the Acoustical Society of America, 2017, 142, 268-275.	1.1	2
240	Theoretical and experimental investigation of the nonlinear dynamics of nanobubbles excited at clinically relevant ultrasound frequencies and pressures: The role of lipid shell buckling. , 2017, , .		2
241	Image Reconstruction Combined With Interference Removal Using a Mixed-Domain Proximal Operator. IEEE Signal Processing Letters, 2018, 25, 1840-1844.	3.6	2
242	K-nearest neighbor classification for the differentiation between freshly excised and decellularized rat kidneys using envelope statistics. , 2018, , .		2
243	Quantitative Ultrasound Imaging for the Differentiation between Fresh and Decellularized Mouse Kidneys*. , 2019, 2019, 6624-6627.		2
244	Fast 3-D Opto-Acoustic Simulation for Linear Array With Rectangular Elements. IEEE Transactions on Ultrasonics, Ferroelectrics, and Frequency Control, 2021, 68, 1885-1906.	3.0	2
245	Acoustic Microscopy of Cells. , 2013, , 315-341.		2
246	Photoacoustic imaging for assessing ischemic kidney damage in vivo. , 2018, , .		2
247	Sound speed estimation in single cells using the ultrasound backscatter power spectrum. Proceedings of Meetings on Acoustics, 2013, , .	0.3	2
248	Characterization of opto-acoustic color mapping for oxygen saturation of blood using biologically relevant phantoms. , 2019, , .		2
249	Real-time non-invasive control of tissue temperature using high-frequency ultrasonic backscattered energy. , 2021, , .		2
250	High frequency ultrasound signal statistics from mouse mammary tissue during involution. , 0, , .		1
251	Examination of contrast mechanisms in optoacoustic imaging of thermal lesions. , 2006, , .		1
252	2G-4 Investigating the Effect of Cell Size on the Backscatter from Suspensions of Varying Volume Fractions. , 2006, , .		1

#	Article	IF	CITATIONS
253	2G-1 Ultrasonic Assessment of Death in HEp2 Cells Using Spectral and Wavelet Based Analysis of Backscattered RF-Signals. , 2006, , .		1
254	Two-dimensional velocity estimation for Doppler optical coherence tomography. , 2007, , .		1
255	Signal analysis for the estimation of mechanical parameters of viable cells using GHz-acoustic microscopy. , 2009, , .		1
256	A simulation study on ultrasound backscattering by cell aggregates with poly-disperse cells. , 2010, , .		1
257	Dynamics of thermoelastic expansion for native and coagulated ex vivo bovine liver tissues. , 2010, , .		1
258	Cell death monitoring using quantitative optical coherence tomography methods. Proceedings of SPIE, 2011, , .	0.8	1
259	Biomechanical properties of soft tissue measurement using optical coherence elastography. Proceedings of SPIE, 2012, , .	0.8	1
260	On the potential of using photoacoustic spectroscopy to monitor red blood cell aggregation. Proceedings of SPIE, 2012, , .	0.8	1
261	Frequency analysis of optoacoustic signals in laser heated tissues. , 2012, , .		1
262	Numerical and experimental classification of the oscillations of single isolated microbubbles: Occurrence of higher order subharmonics. , 2012, , .		1
263	Vaporization, photoacoustic and acoustic characterization of PLGA/PFH particles loaded with optically absorbing materials. , 2013, , .		1
264	In vitro study of PLGA/PFH particles loaded with gold nanoparticles as theranostic agents for photoacoustic imaging and cancer therapy. , 2014, , .		1
265	Circulating tumor cell detection using photoacoustic spectral methods. , 2014, , .		1
266	Identification of red blood cell rouleaux formation using photoacoustic ultrasound spectroscopy. , 2014, , .		1
267	Simultaneous measurement of erythrocyte aggregarion and oxygen saturation under in vitro pulsatile blood flow by high-frequency photoacoustics. , 2014, , .		1
268	Phase Change Nanoemulsions for Cancer Therapy and Imaging. Biophysical Journal, 2015, 108, 332a-333a.	0.5	1
269	Realistic photoacoustic image simulations of collections of solid spheres using linear array transducer. Proceedings of SPIE, 2015, , .	0.8	1
270	Cancer treatment response evaluation using photoacoustic signal envelop statistics: A preliminary study. , 2016, , .		1

#	Article	IF	CITATIONS
271	High frequency photoacoustic spectral analysis of erythrocyte programmed cell death (eryptosis). , 2016, , .		1
272	Single red blood cell oxygenation saturation imaging with multispectral photoacoustic microscopy. , 2016, , .		1
273	Measuring intracellular motion in cancer cell using optical coherence tomography. , 2016, , .		1
274	One-layer microfluidic device for hydrodynamic 3D self-flow-focusing operating in low flow speed. Proceedings of SPIE, 2016, , .	0.8	1
275	Large-pitch steerable synthetic transmit aperture imaging (LPSSTA). , 2016, , .		1
276	Plane-wave imaging using synthetic aperture imaging reconstruction technique with regularized singular-value decomposition (RSVD). , 2016, , .		1
277	Biodegradable polymer based theranostic agents for photoacoustic imaging and cancer therapy. , 2016, , .		1
278	Noninvasive tissue temperature estimation using nonlinear ultrasound harmonics. AIP Conference Proceedings, 2017, , .	0.4	1
279	Ultrasound spectral analysis of photoacoustic signals from red blood cell populations at different optical wavelengths. Proceedings of SPIE, 2017, , .	0.8	1
280	Photoacoustic ToF tomography of blood cells: From mathematical approximation to super-resolution. , 2017, , .		1
281	Preliminary photoacoustic imaging of the human radial artery for simultaneous assessment of red blood cell aggregation and oxygen saturation in vivo. , 2017, , .		1
282	Structurally random Fourier domain compressive sampling and frequency domain beamforming for ultrasound imaging. , 2017, , .		1
283	Enhancing fluorescein distribution from in situ forming PLGA implants using therapeutic ultrasound. , 2017, , .		1
284	Structurally enhanced contrast in photoacoustic microscopy with F-Mode imaging. , 2017, , .		1
285	Using ultrasound and photoacoustics to monitor in situ forming implant structure and drug release. , 2017, , .		1
286	High-Frame Rate 3D-Synthetic Transmit Aperture Imaging with a Reduced Number of Measurement Channels. , 2018, , .		1
287	Sizing Cells Using Acoustic Flow Cytometry. , 2018, , .		1
288	Nanobubble Facilitated Optoporation and Photoacoustic Imaging of BT-474 Breast Cancer Cells. , 2018, , .		1

#	Article	IF	CITATIONS
289	Zonyl FSP fluorosurfactant stabilized perfluorohexane nanoemulsions as stable contrast agents. , 2019, , .		1
290	Investigating the Kinetics of Blood Coagulation using Ultrasound. , 2019, , .		1
291	Photoacoustic measurements of red blood cell oxygen saturation in blood bags in situ. Proceedings of SPIE, 2017, , .	0.8	1
292	Measuring the nucleus-to-cytoplasmic ratio in PC-3 cells using photoacoustic flow cytometry and imaging flow cytometry. , 2019, , .		1
293	Comparison of measurements of the nucleus-to-cytoplasmic ratio in MCF-7 cells using ultra-high frequency photoacoustic microscopy and imaging flow cytometry. , 2019, , .		1
294	An ultrafast enzyme-free acoustic technique for detaching adhered cells in microchannels. RSC Advances, 2021, 11, 32824-32829.	3.6	1
295	Quantitative Ultrasound and Cell Death. , 2013, , 95-115.		1
296	Ultrasound Imaging of DNA-Damage Effects in Live Cultured Cells and in Brain Tissue. Methods in Molecular Biology, 2017, 1644, 23-40.	0.9	1
297	Acoustic and Photoacoustic Inspection of Through-Silicon Vias in the CHz-Frequency Band. , 2017, , .		1
298	Spectroscopic photoacoustics for assessing ischemic kidney damage. , 2018, , .		1
299	Simultaneous ultrasound and photoacoustics based flow cytometry. , 2018, , .		1
300	Pharmacokinetic Modeling of the Second-Wave Phenomenon in Nanobubble-Based Contrast-Enhanced Ultrasound. IEEE Transactions on Biomedical Engineering, 2023, 70, 42-54.	4.2	1
301	Ultrasound Biomicroscopy as a Probe of Cellular Ultrastructure. Microscopy and Microanalysis, 2002, 8, 1028-1029.	0.4	0
302	P3E-3 Finite Element Modeling of Ultrasound Scattering by Spherical Objects and Cells. , 2006, , .		0
303	P6C-4 Extended System Transfer Compensation for Parametric Imaging in Ultrasonic Response Assessment of Anti-Cancer Therapies. Proceedings IEEE Ultrasonics Symposium, 2007, , .	0.0	0
304	P3D-3 Transmission Ultrasound Imaging to Guide Thermal Therapy. Proceedings IEEE Ultrasonics Symposium, 2007, , .	0.0	0
305	Monitoring Responses to Treatment With High-Frequency Ultrasound In Vivo: Assessing Response to Radiation vs. Photodynamic Therapy in Melanoma Xenograft Tumors. International Journal of Radiation Oncology Biology Physics, 2007, 69, S69-S70.	0.8	0
306	Novel Low-frequency Ultrasound Monitoring of Tumor Cell Death in Response to Therapy. International Journal of Radiation Oncology Biology Physics, 2008, 72, S684.	0.8	0

#	Article	IF	CITATIONS
307	A novel technique for measuring ultrasound backscatter from single micron-sized objects. , 2009, , .		Ο
308	A Monte Carlo study on the effects of erythrocyte oxygenation on photoacoustic signals. , 2011, , .		0
309	Simultaneous photoacoustic detection of red blood cell aggregation and oxygenation. , 2012, , .		0
310	Nonlinear dynamics of polymer shell ultrasound contrast agents at 8–32 MHz ultrasonic excitations. , 2013, , .		0
311	Classifying normal and abnormal vascular tissues using photoacoustic signals. , 2013, , .		0
312	Photoacoustic assessment of oxygen saturation: effect of red blood cell aggregation. Proceedings of SPIE, 2013, , .	0.8	0
313	Optical coherence tomography detection of shear wave propagation in layered tissue equivalent phantoms. Proceedings of SPIE, 2013, , .	0.8	0
314	Acoustic and photoacoustic imaging of spheroids. Proceedings of Meetings on Acoustics, 2013, , .	0.3	0
315	From high-frequency to low-frequency cell death detection: quantitative ultrasound evaluation of tumor response in breast cancer. Proceedings of Meetings on Acoustics, 2013, , .	0.3	0
316	Ultra-high frequency acoustic impedance maps of MCF-7 cells. , 2014, , .		0
317	Effective scatterer size estimates in HT-29 spheroids at 55 MHz and 80 MHz. , 2014, , .		0
318	Detecting apoptosis in vivo and ex vivo using spectroscopic OCT and dynamic light scattering. , 2014, , .		0
319	Temperature dependence of harmonics generated by nonlinear ultrasound beam propagation in water: A simulation study. , 2014, , .		0
320	Optical coherence tomography detection of shear wave propagation in MCF7 cell modules. , 2014, , .		0
321	Reducing the number of receiving channels using transmit-receive symmetry in synthetic transmit aperture imaging. , 2015, , .		0
322	Multifunctional perfluorocarbon nanoemulsions for cancer therapy and imaging. , 2015, , .		0
323	High-frequency photoacoustic imaging of erythrocyte aggregation and oxygen saturation: probing hemodynamic relations under pulsatile blood flow. , 2015, , .		0
324	Low power continuous wave photoacoustic microscope for bioimaging applications. , 2015, , .		0

#	Article	IF	CITATIONS
325	Acoustic and photoacoustic microscopy imaging of single leukocytes. , 2016, , .		Ο
326	Photoacoustic radiofrequency spectroscopy for monitoring cancer treatment response. , 2016, , .		0
327	High frequency ultrasound imaging and spectral analysis of sea urchin oocytes. , 2016, , .		Ο
328	Ultrasound and photoacoustic analysis of cell pellets at 200 MHz. , 2016, , .		0
329	Steering the receiving field of view (FOV) without applying delays insynthetic transmit aperture imaging (STA). , 2016, , .		0
330	Photoacoustic spectral analysis to sense programmed erythrocyte cell death (eryptosis) for monitoring cancer response to treatment. Proceedings of SPIE, 2016, , .	0.8	0
331	Visualization and characterization of the acoustic radiation force assisted displacement of particles using an OCT technique (Conference Presentation). , 2016, , .		Ο
332	Photoacoustic simulation of microvessel bleeding: spectral analysis and its implication for monitoring vascular-targeted treatments. , 2016, , .		0
333	Monitoring cancer treatment response using photoacoustic and ultrasound spectral analysis in combination with oxygenation measurements (Conference Presentation). , 2016, , .		Ο
334	Photoacoustic investigation of gold nanoshells for bioimaging applications. , 2016, , .		0
335	Ultrasound Imaging of Apoptosis: Spectroscopic Detection of DNA-Damage Effects In Vivo. Methods in Molecular Biology, 2017, 1644, 41-60.	0.9	Ο
336	Photoacoustic detection of cancer cells using targeted gold nanorod loaded PLGA nanoparticles. , 2017, , .		0
337	A preliminary study of the mean scatterer spacing estimation from pellets using wavelet-based cepstral analysis. , 2017, , .		0
338	Microfluidic shrinking of microbubble contrast agents. , 2017, , .		0
339	Structurally enhanced contrast in photoacoustic microscopy with F-mode imaging. , 2017, , .		0
340	Using ultrasound and photoacoustics to monitor in situ forming implant structure and drug release. , 2017, , .		0
341	Characterization of the In-Vivo Uptake of Novel Contrast Agents Using Photoacoustic Radiofrequency Spectra. , 2018, , .		0
342	Simulation of Photoacoustic Imaging of Red Blood Cell Aggregation Using a Numerical Model of		0

Pulsatile Blood Flow. , 2018, , .

#	Article	IF	CITATIONS
343	Radiation-enhanced nanobubble therapy: Monitoring treatment effects using photoacoustic imaging. , 2019, , .		0
344	Differential frequency-domain photoacoustic microscope for blood oxygen saturation measurements. , 2019, , .		0
345	Acoustic Microflows: Dancing with the Cells: Acoustic Microflows Generated by Oscillating Cells (Small 9/2020). Small, 2020, 16, 2070045.	10.0	0
346	3-D Large-Pitch Synthetic Transmit Aperture Imaging With a Reduced Number of Measurement Channels: A Feasibility Study. IEEE Transactions on Ultrasonics, Ferroelectrics, and Frequency Control, 2021, 68, 1628-1640.	3.0	0
347	Ultrasonic detection of anti cancer treatment success using tissue acoustic properties and parametric imaging. , 0, , .		0
348	Quantitative Optical Coherence Tomography Imaging of Cell Death. , 2010, , .		0
349	Shear-wave generation using acoustic radiation force detected by Optical Coherence Elastography. , 2012, , .		0
350	Acoustical imaging of internal spheroid structures for a series of frequencies. Proceedings of Meetings on Acoustics, 2013, , .	0.3	0
351	An analysis of the acoustic properties of the cell cycle and apoptosis in MCF-7 cells. Proceedings of Meetings on Acoustics, 2013, , .	0.3	0
352	Abstract LB-165: Early detection of the therapeutic effect in tumors treated with a thermosensitive liposome (TSL) using noninvasive ultrasound and photoacoustic imaging. , 2014, , .		0
353	Multispectral photoacoustic bioimaging using low power continuous wave lasers. , 2017, , .		0
354	Rapid computation of photoacoustic fields from normal and pathological red blood cells using a Green's function method. Proceedings of SPIE, 2017, , .	0.8	0
355	Spatial interference encoding patterns based super resolved photoacoustic microscopy. , 2017, , .		Ο
356	Correlations in photoacoustic estimates of tumor oxygenation during novel cancer therapies with power Doppler measurements (Conference Presentation). , 2017, , .		0
357	Individual nanobubbles detection using acoustic based flow cytometry. , 2019, , .		Ο
358	Investigation of the thermal properties of biological cells using a frequency domain photoacoustic microscope. , 2019, , .		0
359	Dye diffusion proximal to in situ forming implants is increased by ultrasound stimulation. , 2020, , .		0
360	Effects of shell-integrated Sudan Black dye on the acoustic activity and ultrasound imaging properties of lipid-shelled nanoscale ultrasound contrast agents. Journal of Biomedical Optics, 2022, 27, .	2.6	0